Electronic Supplementary Material (ESI) for Materials Chemistry Frontiers.

Supporting Information

Palladium-Based Metal-Organic Coordination Nanoparticles for Efficient Tumor Treatment via Synergistic Enhancement of ROS Production

Chang Liu,[ab] Na Yang,[ab] Mengyao Li,[ab] Shuang Song,[a] Wei Zhou,[ab] Jia Ren,[ab] Di Demi He,[a] Wenzhao Han,[a] Ying Li[a] and Cong Yu*[ab]

[a] State Key Laboratory of Electroanalytical Chemistry, Changchun Institute of Applied Chemistry, Chinese Academy of Sciences, Changchun, 130022, China

[b] University of Science and Technology of China, Hefei, 230026, China

*Corresponding author E-mail address: congyu@ciac.ac.cn

Experimental section

1.1 Materials

K_2PdCl_4, Rose Bengal (RB), β-lapachone (LAP), polyvinyl pyrrolidone (PVP), hydrogen peroxide (H_2O_2), 1,3-diphenylisobenzofuran (DPBF), terephthalic acid (TA) and 3,3′,5,5′-tetramethylbenzidine (TMB) were acquired from Shanghai Macklin Biochemical Co., Ltd. 9,10-Anthracenediyl-bis(methylene)dimalonic acid (ABDA), dicoumarol were purchased from Bide Pharmatech Ltd. DMEM medium, trypsin-EDTA, fetal bovine serum (FBS), and 2′,7′-dichlorofluorescein diacetate (DCFH-DA) were obtained from Gibco Life Technologies. The primary antibodies targeting β-actin

were sourced from Wuhan Servicebio Technology Co., Ltd., the secondary antibodies of HRP Goat Anti-Mouse IgG H&L and HRP Goat Anti-Rabbit IgG H&L, were also procured from the same supplier. The primary antibodies for NQO1 were obtained from Cell Signaling Technology. Cell Counting Kit-8 (CCK-8) and Calcein-AM/PI double staining kit were provided by Promega Biotech Co., Ltd. All other chemicals utilized in this study were of analytical reagent grade and used without further processing steps. Millipore deionized water (18.2 MΩ/cm, 25 °C) was employed to prepare all sample solutions.

1.2 Characterization

H-600 electron microscope (TEM, Hitachi, Japan) was used to characterize morphology of the Pd@RB NPs and the Pd@RB@LAP NPs. Cary 50 Bio Spectrophotometer (Varian Inc., CA, USA) was used to record the UV-vis absorption spectra. X-ray photoelectron (XPS) characterizations were carried out on a Thermo Scientific ESCALAB 250Xi X-ray photoelectron spectroscopy (USA). Confocal laser scanning microscope (CLSM) images were obtained using a Nikon ECLIPSE Ti microscope (Japan).

1.3 Cell culture

293T, L929, L-02, MCF-7, Hela, A549, HepG2 and 4T1 cells were cultured in high glucose DMEM containing 10% fetal bovine serum and 1% penicillin-streptomycin solution under a humidified 5% carbon dioxide at 37 °C.

1.4 Intracellular ROS detection

To evaluate the intracellular ROS levels, we employed DCFH-DA as the probe. 4T1 cells were plated in 6-well plates (1×10^5 per well). They were then incubated in the dark with DMEM media containing PBS, RB (43.25 μg/mL), LAP (6.75 μg/mL), Pd@RB NPs (43.25 μg/mL), and Pd@RB@LAP NPs (50 μg/mL), respectively, for 3 h. The original media were replaced with a staining solution of DCFH-DA (10 μM), and the assay solutions were incubated for an additional 20 min. In the laser group, cells were subjected to laser irradiation (538 nm, 0.5 W/cm^2) for 10 min. Conversely, the no-laser control group was cultured in the dark. Finally, all cells were imaged through CLSM.

In order to further verify the enhancement effect of LAP on ROS production, dicoumarol (50×10^{-6} M) was added to cells treated with different materials, and the fluorescence images were collected. Finally, ROS production in normal L929 and 239T cells was observed using the same experimental steps as mentioned above.

1.5 Western blot analysis of NQO1 production

Western blot analysis was employed to explore the upregulation of NQO1 expression by ROS. 4T1 cells were cultured on 6-cm dishes at a density of 2×10^5 cells overnight. The incubation media was then replaced with fresh medium containing free RB (43.25 μg/mL), free LAP (6.75 μg/mL), Pd@RB NPs (43.25 μg/mL), and Pd@RB@LAP NPs (50 μg/mL), respectively. Following 6 h of incubation, the laser group was exposed to 538 nm laser (0.5 W/cm^2) for 10 min. Fresh medium without laser irradiation was used as the control. Cells were collected after an additional 6 h of incubation and lysed with

RIPA buffer to extract protein samples. Subsequently, proteins were analyzed using 10% SDS-PAGE. After incubation with antibodies specific for NQO1 or β-actin, protein bands were analyzed with a ChemiScope 6100 Touch luminescence imaging system.

1.6 In vitro cytotoxicity assay

4T1 cells were first grown in 96-well plates (1×10^4 per well). Following a 24-hour incubation period, these cells were subjected to varying concentrations of RB, LAP, Pd@RB NPs, and Pd@RB@LAP NPs, respectively, for another 24 h. For the laser groups, a 538 nm laser (0.5 W/cm^2) was applied for 5 min. The no-laser control group remained in darkness. To evaluate cell viability, the CCK-8 assay was performed. The concentrations of the Pd@RB@LAP NPs were 0, 10, 20, 30, 40, 50, and 60 μg/mL, respectively; the concentrations of RB and the Pd@RB NPs were both of 8.65, 17.3, 25.95, 34.6, 43.25, and 51.9 μg/mL, respectively; and the concentrations of LAP were 1.35, 2.7, 4.05, 5.4, 6.75, and 8.1 μg/mL, respectively. All materials were added based on the loading content of LAP in Pd@RB@LAP NP. 293T, L929, L-02, MCF-7, A549, HepG2 and Hela cells were treated using the same procedures.

1.7 In vitro anti-tumor effect

4T1 cells were placed in 6-well plates (1×10^5 per well) and incubated with PBS, RB (43.25 μg/mL), LAP (6.75 μg/mL), the Pd@RB NPs (43.25 μg/mL), and the Pd@RB@LAP NPs (50 μg/mL) for 4 h. After that, the laser groups were subjected to 538 nm laser (0.5 W/cm^2) irradiation for 10 min, and incubated for another 12 h. After

that, the culture medium was removed and the plate rinsed, cells were stained using a solution of calcein acetoxymethyl ester (calcein AM, 2 μM) and propidium iodide (PI, 4 μM) and incubated for 20 min more. After rinsed with PBS, the cells were imaged using CLSM. The Calcein-AM and PI were excited with lasers at 488 and 561 nm, respectively.

1.8 Hemolysis assay

Mouse whole blood was centrifuged at 3000 rpm for 5 min and washed five times with PBS to get pure erythrocytes. Afterwards, 1% erythrocytes (v/v) were incubated with the Pd@RB@LAP NPs solution at various concentrations (10, 20, 30, 40, 50, and 60 μg/mL) at 37 °C for 4 h. Erythrocytes mixed with pure water served as a positive control, and those mixed with PBS served as a negative control. The samples were centrifuged and the absorbance of the supernatants at 540 nm were measured using a microplate reader. The percentage of hemolysis was calculated using the following equation:[S1]

$$\text{Hemolysis (\%)} = (A_{sample} - A_{negative}) / (A_{positive} - A_{negative}) \times 100\%$$

Where A_{sample}, $A_{negative}$, and $A_{positive}$ refer to the absorption of material sample solution, PBS, and H_2O at 540 nm, respectively.

1.9 In vivo anti-tumor effect

Female BALB/c mice bearing 4T1 were allocated into six groups, with five mice in each group (PBS, LAP, Pd@RB NPs, Pd@RB NPs + Laser, Pd@RB@LAP NPs, Pd@RB@LAP NPs + Laser). The treatment groups received intratumor injections of

LAP (1.62 mg/kg), the Pd@RB NPs (10.38 mg/kg), and the Pd@RB@LAP NPs (12 mg/kg) in PBS buffer on days 1, 3, and 5, respectively, while the control group received only PBS buffer injections. 24 h after administration, the tumors of the Pd@RB NPs + Laser and the Pd@RB@LAP NPs + Laser groups were irradiated with 538 nm laser (0.5 W/cm^2) for 10 min. Tumor volume and body weight of the mice were measured every 2 days. The tumor volume was determined using the equation: tumor volume = (tumor length) × (tumor width)^2/2. On day 14, all mice were euthanized and their major organs and tumors were collected for western blot, H&E and DHE analysis.

All animal experimental protocols have been approved by the Animal Welfare and Ethics Committee of Changchun Institute of Applied Chemistry, Chinese Academy of Sciences (IACUC Issue Number: CIAC20230172).

1.10 Statistical Analysis

All experiments were performed at least 3 times, and the results were expressed as means ± standard deviation (SD). One-way single-factor analysis of variance (ANOVA) was carried out to determine the statistical significance of the data. Statistical analyses were conducted and obtained using GraphPad Prism 9.0 software. Statistically significant differences were denoted by ns $p > 0.05$, *$p < 0.05$, **$p < 0.01$, ***$p < 0.001$, and **** $p < 0.0001$ respectively.

Supplementary Figures

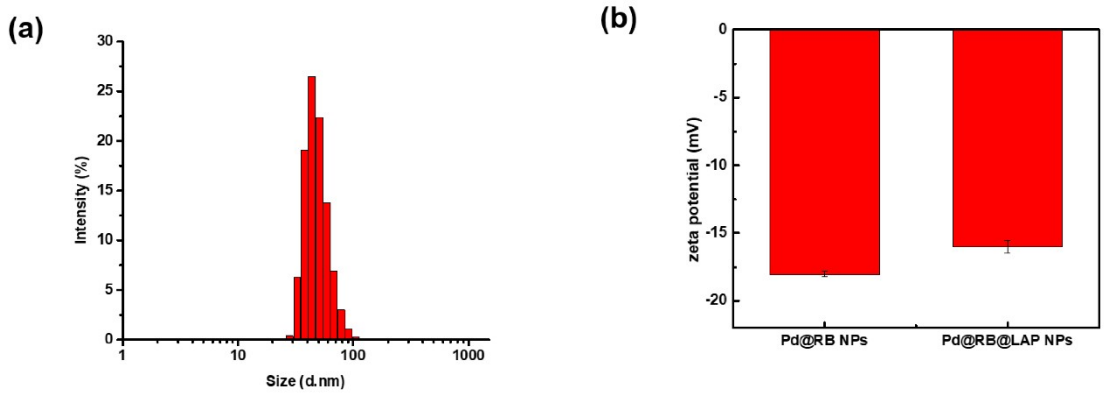

Fig. S1 (a) DLS size distribution of the Pd@RB@LAP NPs. (b) Zeta potential values of the Pd@RB NPs and the Pd@RB@LAP NPs.

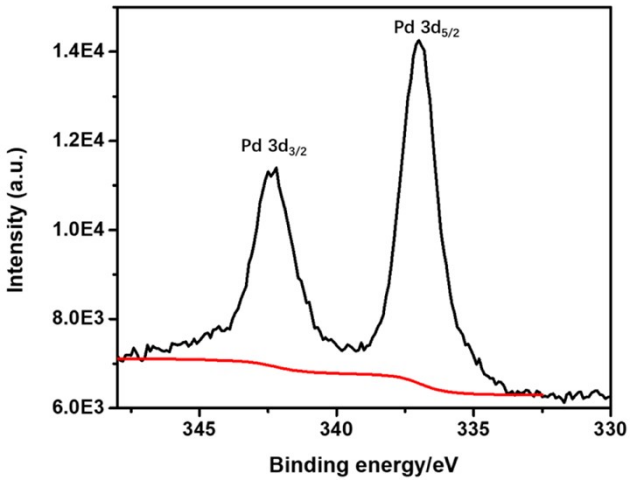

Fig. S2 XPS spectrum of the Pd@RB@LAP NPs showing the Pd 3d bands.

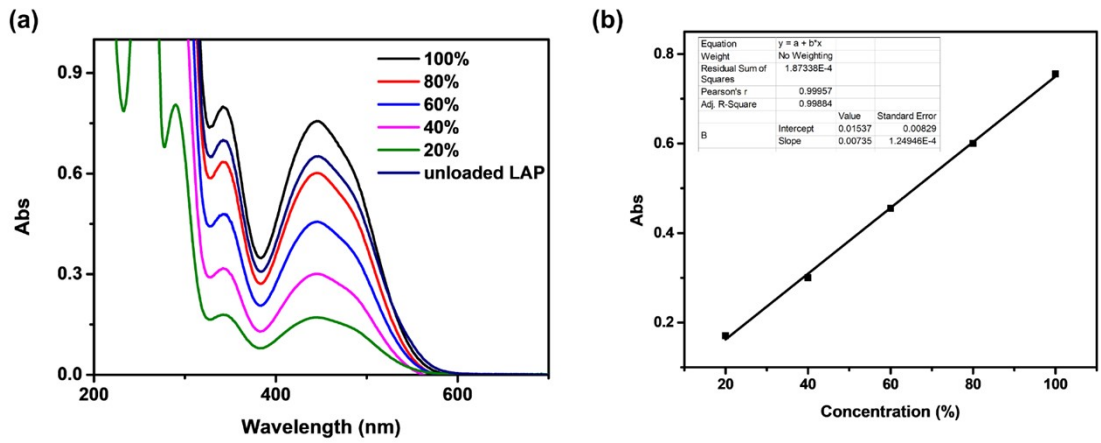

Fig. S3 (a) UV-vis absorption spectral changes of different amounts of LAP. (b) The standard curve for LAP quantification. UV-vis absorption intensity at 448 nm was plotted against LAP content.

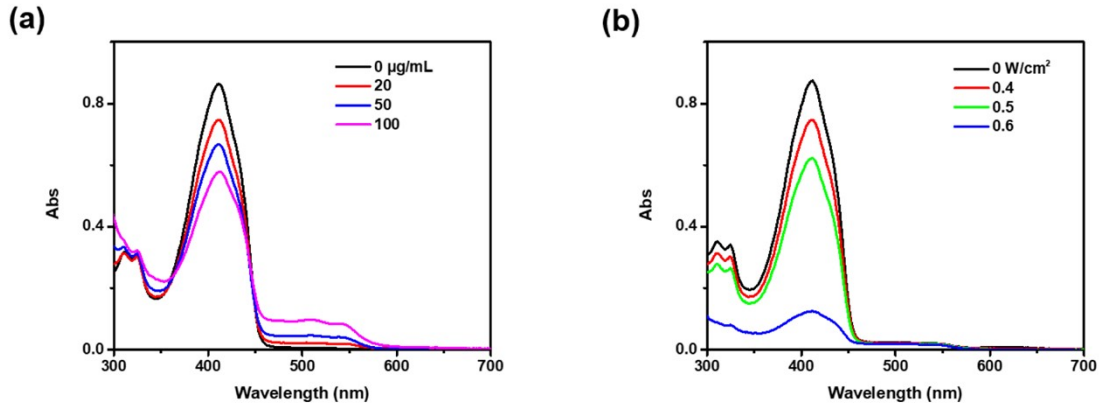

Fig. S4 (a) Absorption spectral changes of DPBF when treated with various concentrations of the Pd@RB@LAP NPs and under 538 nm laser irradiation (0.5 W/cm^2) for 30 s. (b) Absorption spectral changes of DPBF when treated with the Pd@RB@LAP NPs (50 μg/mL) and under laser irradiation at different power densities for 30 s.

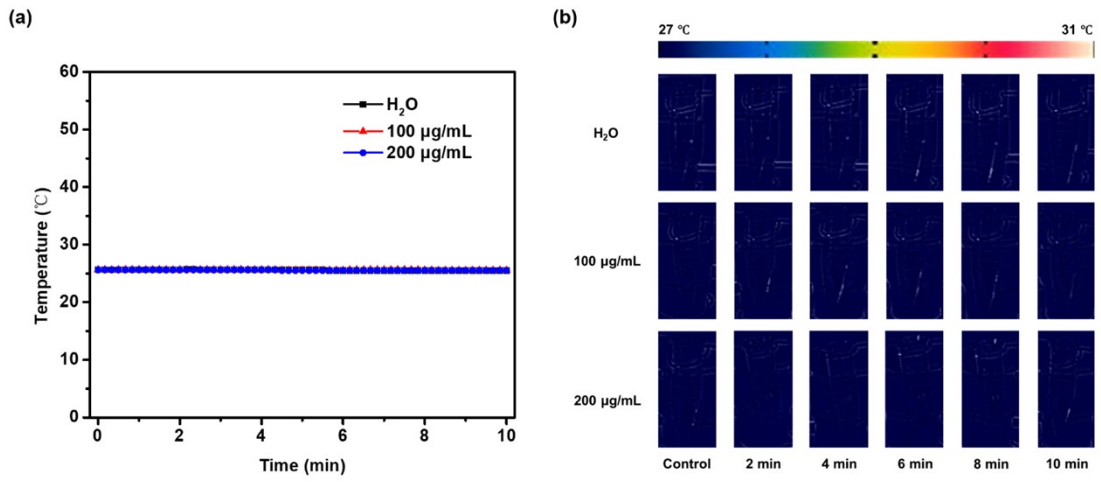

Fig. S5 (a) Temperature changes with time and (b) Real-time thermographic images of the Pd@RB@LAP NPs sample solutions at different concentrations and under 538 nm laser irradiation (1.5 W/cm^2).

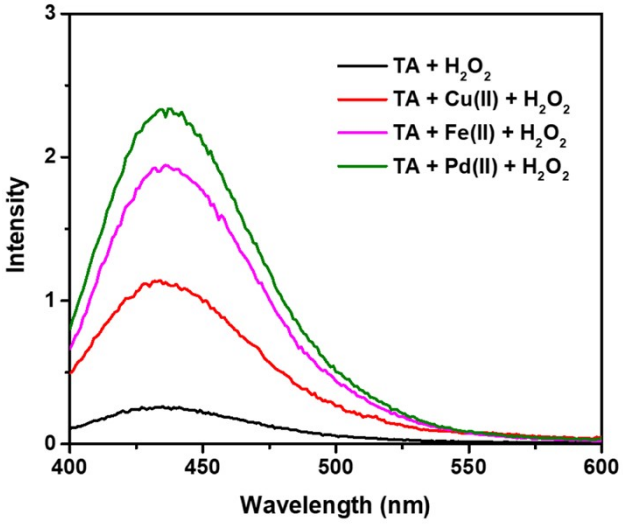

Fig. S6 Fluorescence spectral changes of TA after treated with different metal ions (50 μM) at pH 6.5 for 10 min.

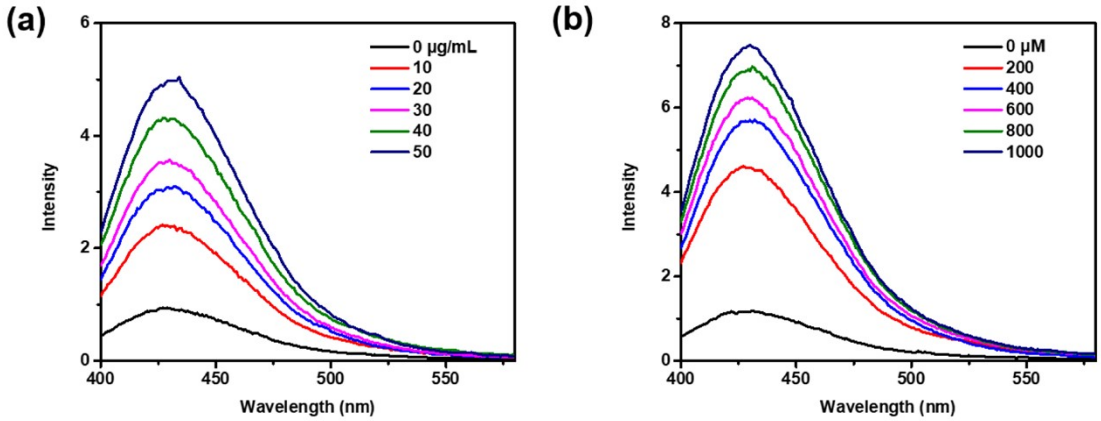

Fig. S7 (a) Fluorescence spectral changes of TA when treated with various concentrations of the Pd@RB@LAP NPs and in the presence of 200 μM H_2O_2 for 30 min. (b) Fluorescence spectral changes of TA when treated with different concentrations of H_2O_2 in the presence of 50 μg/mL Pd@RB@LAP NPs for 30 min.

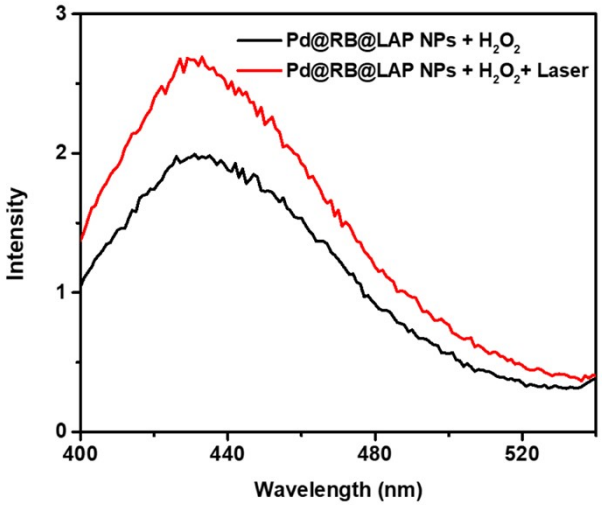

Fig. S8 Changes in fluorescence spectra of TA when mixed with the Pd@RB@LAP NPs (50 μg/mL) and with/without 10 min laser irradiation.

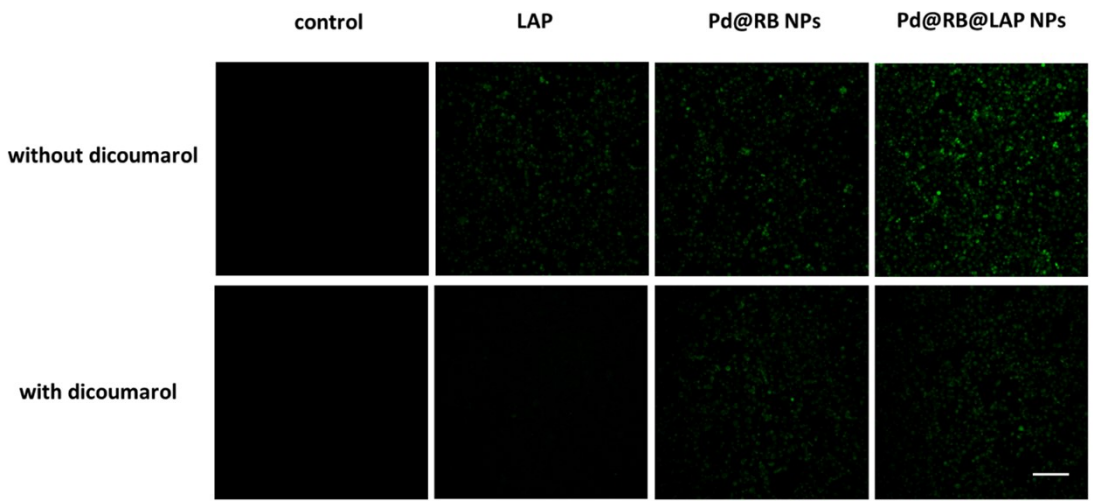

Fig. S9 Intracellular ROS detection by DCFH-DA. 4T1 cells were treated with LAP, the Pd@RB NPs and the Pd@RB@LAP NPs in the absence or presence of dicoumarol (50×10^{-6} M). Scale bar, 200 μm.

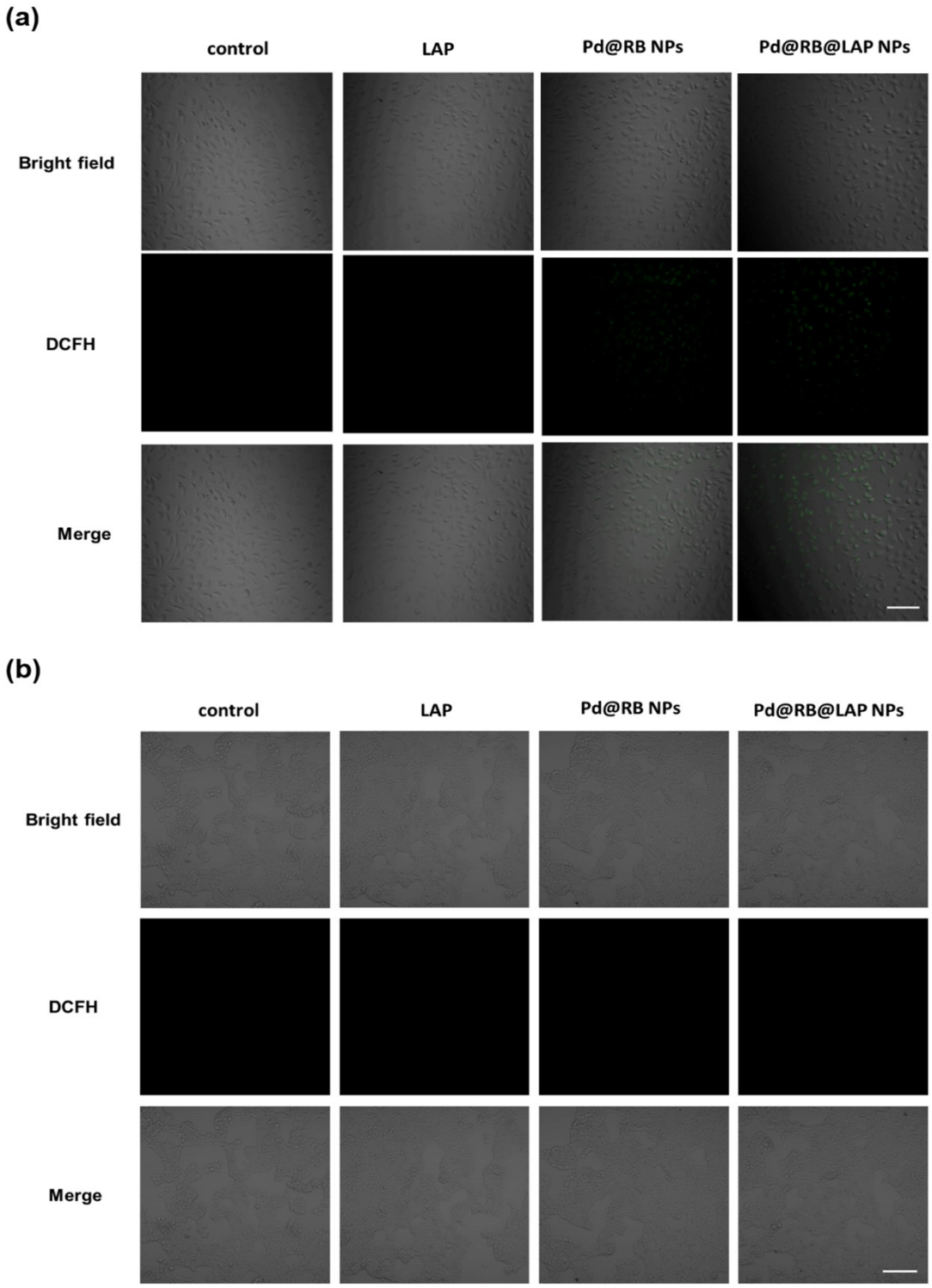

Fig. S10 Intracellular ROS detection by DCFH-DA. (a) L929 and (b) 293T cells were treated with LAP, the Pd@RB NPs and the Pd@RB@LAP NPs. Scale bar, 200 μm.

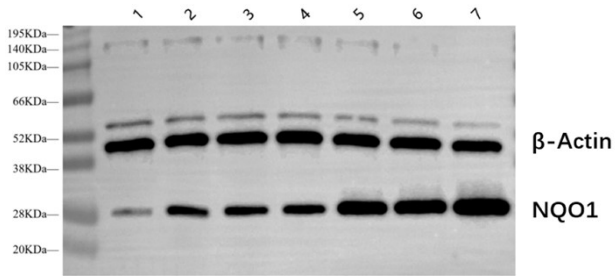

Fig. S11 The picture of whole blots. 1, Control; 2, RB + Laser; 3, LAP; 4, Pd@RB NPs; 5, Pd@RB NPs + Laser; 6, Pd@RB@LAP NPs; 7, Pd@RB@LAP NPs + Laser.

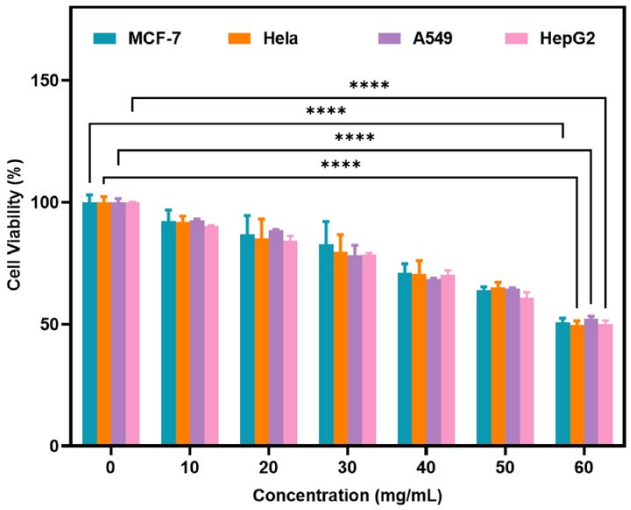

Fig. S12 Cytotoxicity of the Pd@RB@LAP NPs towards MCF-7, Hela, A549 and HepG2 cells in the dark. Statistical significances were calculated using one-way ANOVA (ns $p > 0.05$, *$p < 0.05$, **$p < 0.01$, ***$p < 0.001$, ****$p < 0.0001$).

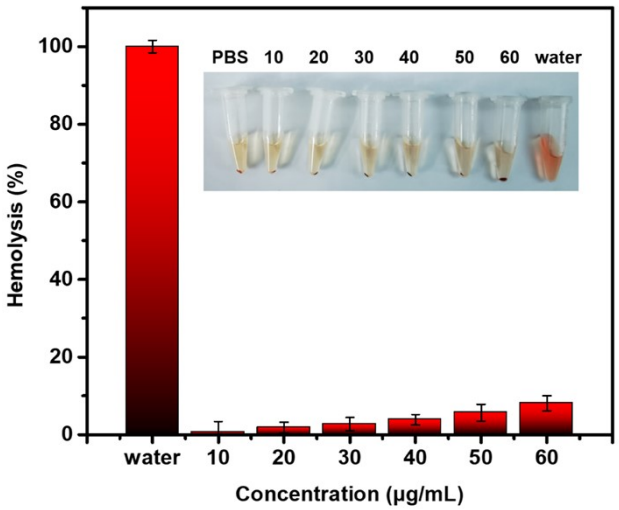

Fig. S13 Hemolysis value of the Pd@RB@LAP NPs at different concentrations. Inset shows the image of the corresponding hemolysis sample solutions.

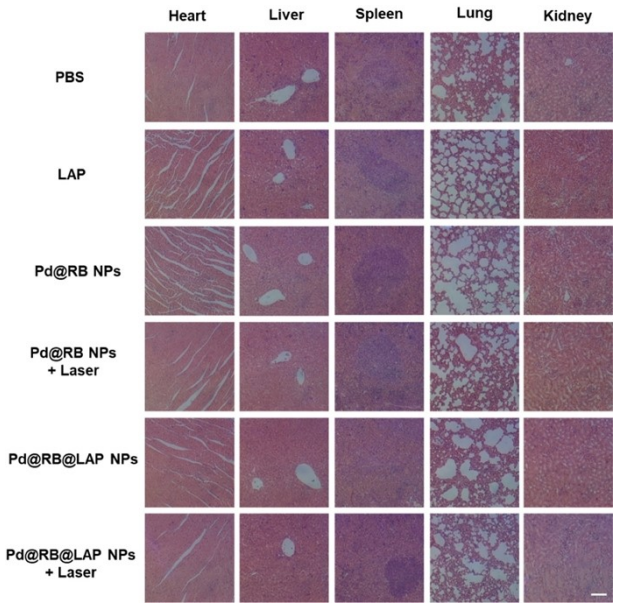

Fig. S14 H&E staining of the slices of major organs (heart, liver, spleen, lung, and kidney) of the mice under different treatments. Scale bar, 100 μm.

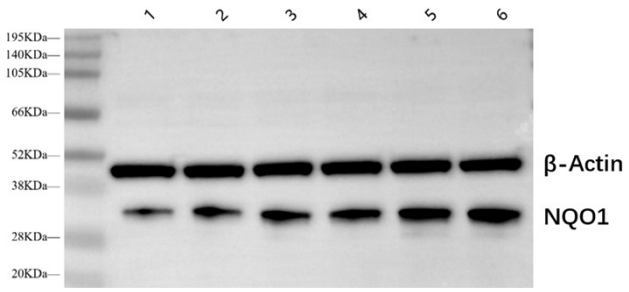

Fig. S15 The picture of whole blots of NQO1 in tumor tissues. 1, Control; 2, LAP; 3, Pd@RB NPs; 4, Pd@RB NPs + Laser; 5, Pd@RB@LAP NPs; 6, Pd@RB@LAP NPs + Laser.

Reference

S1 Q. Gao, D. Huang, Y. Deng, W. Yu, Q. Jin, J. Ji and G. Fu, Chlorin e6 (Ce6)-loaded supramolecular polypeptide micelles with enhanced photodynamic therapy effect against Pseudomonas aeruginosa, *Chem. Eng. J.*, 2021, **417**, 129334.